

Modeling of board-level package by Finite Element Analysis and laser interferometer measurements

Bo Zhang^a, Pin-kuan Liu^{a,*}, Han Ding^a, Wenwu Cao^b

^a State Key Laboratory of Mechanical System and Vibration, School of Mechanical Engineering, Shanghai Jiao Tong University, 800 Dong Chuan Road, Shanghai 200240, China

^b Materials Research Institute, The Pennsylvania State University, University Park, PA 16802, USA

ARTICLE INFO

Article history:

Received 12 November 2009

Received in revised form 16 March 2010

ABSTRACT

Board-level package is a complicated multi-components structure. It can be simulated by an equivalent Finite Element Analysis (FEA) model of the board-level package, in which detailed layer structure of the Print Circuit Board (PCB), signal wires and through-holes were ignored. For this purpose, it is necessary to obtain the equivalent material properties of the board-level package. In this work, a laser-based interferometric technique was used to measure the modal parameters of the board-level package. By fitting the FEA results with the experimental results, we can obtain equivalent material properties of the board-level package by means of the Taguchi method. Four control factors (Young's modulus in the x and y direction, mass density and shear modulus in the xy plane) at three levels are explored and assigned to the columns of a $L_9(3^4)$ saturated orthogonal array. The so obtained equivalent parameters provided the best fit between the FEA results and the experimental observations.

Crown Copyright © 2010 Published by Elsevier Ltd. All rights reserved.

1. Introduction

Multi-functionalities and miniaturization of portable electronic products make the anti-drop performance of solder interconnections a vital issue in modern electronic industry. It is difficult to measure the dynamic response of solder interconnections during drop tests due to their small dimension and fine pitch. Finite Element Analysis (FEA) has been proven an effective way to study the dynamic stress and strain response of the solder interconnections [1–9].

However, it is difficult to build a detailed finite element (FE) model of the board-level package due to the complicated structure involved, such as the layer structure, through-holes and signal wires of the Print Circuit Board (PCB). In order to reduce the size of the FE model, it is necessary to build an equivalent FE model with equivalent material properties. The accuracy of the FEA solution greatly depends on the input equivalent material properties of the board-level package.

Modal analysis is the base for the analysis of the dynamic response of the board-level package when mode superposition method is adopted. The inherent properties of the board-level package, including modal deflection contour, natural frequency and structural damping, can be obtained by Experimental Modal Analysis (EMA). The EMA results can be used to verify the equivalent FE

model of the board-level package and optimize the equivalent material properties.

Modal analysis of board-level package had been studied by the hammer method. Lee et al. [10] performed the EMA to establish an equivalent FE model for the dynamic response analysis of the board-level package. Zhang et al. [11] also carried out the modal analysis of the board-level package by theoretical and experimental analyses. However, the added-mass of the accelerometer and hammer greatly decreased the test accuracy because the added-mass cannot be ignored compared to the mass of the board-level package. In addition, due to the low stiffness coefficient of the board-level package, it is difficult to obtain a good coherence function at some positions (e.g., the edge of board-level package). The narrow bandwidth of the input pulse by the hammer also leads to poor coherence functions in the high frequency region. On the other hand, the laser-based interferometric technique is a non-contact, full-field and real-time test method [12], and thus a much better method for the modal parameter test of small and light objects.

In this paper, we used the laser-based interferometric technique to measure the modal parameters of the board-level package with two opposed edges fixed and another two opposed edges free. The mode shapes and natural frequencies of the board-level package were experimentally measured using Optonor VibroMap 1000 system based on the technology of TV-holography. The equivalent FE model of the board-level package was built using ANSYS and the equivalent material properties were obtained by optimizing the matching between FEA and EMA results.

* Corresponding author. Tel./fax: +86 21 34207143.

E-mail address: pkliu@sjtu.edu.cn (P.-k. Liu).

2. Experimental setup

The IC component, including 108 joints of Sn–3.5Ag–0.7Cu solder, with the dimension of 11 mm × 13 mm × 0.9 mm, is a stacked-die Chip Scale Package (CSP). The pad on the substrate has solder-mask-defined structural configuration. The surface finish of the Cu substrate pad is coated with plated Ni/Au and the solder joints with the diameter of 0.36 mm are placed on the substrate with a pitch of 0.8 mm. Three CSP samples are assembled on an eight-layer PCB with the dimension of 132 mm × 77 mm × 1 mm, and located at position U3, U8 and U13 as labeled in Fig. 1. The total weight of the board-level package is about 23.80 g. The Cu pad on the test board also has solder-mask-defined structural configuration. The Cu pad has Organic Solderability Preservatives (OSP) as surface finish and non-via-in-pad structure is adopted.

Fig. 2 shows the experimental setup used to measure the modal properties of the board-level package, which includes the following: personal computer (PC), analog video filter, Optonor VibroMap 1000, board-level package, clamp, B&K exciter, 2706 power amplifier, DAC and a monitor. Fig. 3 shows the spot of modal test.

The Optonor VibroMap 1000 based on laser interferometric technique is a non-contact and full field vibration measuring system [12]. It could measure the surface vibration of an object with the dimension from several millimeters to several meters. The object is illuminated by an expanded beam and imaged by a built-in video system in VibroMap 1000. The surface vibration of the object

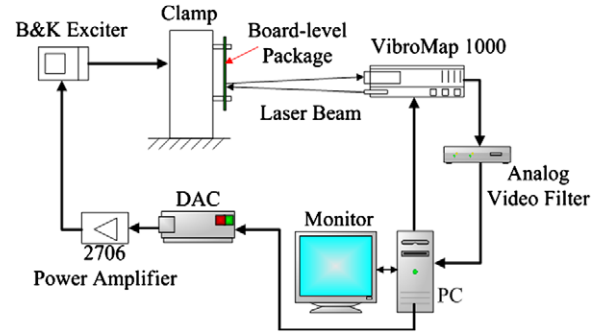


Fig. 2. Setup of the test system.

is detected by an internal reference laser beam which interferes with the object light. The VibroMap 1000 measures the vibration one frequency at a time. After the filtering process by an Analog Video Filter, the measured images are transmitted to a PC, then, numerical values of the amplitude and phase distributions were calculated and 2D graphics, including an animated display of the vibration, were generated. The object excitation is controlled by the computer and the DAC converts the frequency and amplitude of the excitation pulse from digital format into analog format. The excitation pulse magnified by a 2706 power amplifier drives the B&K exciter. The excitation signal is sinusoidal, and the amplitude of the force excitation pulse is 29.4 N with the frequency var-

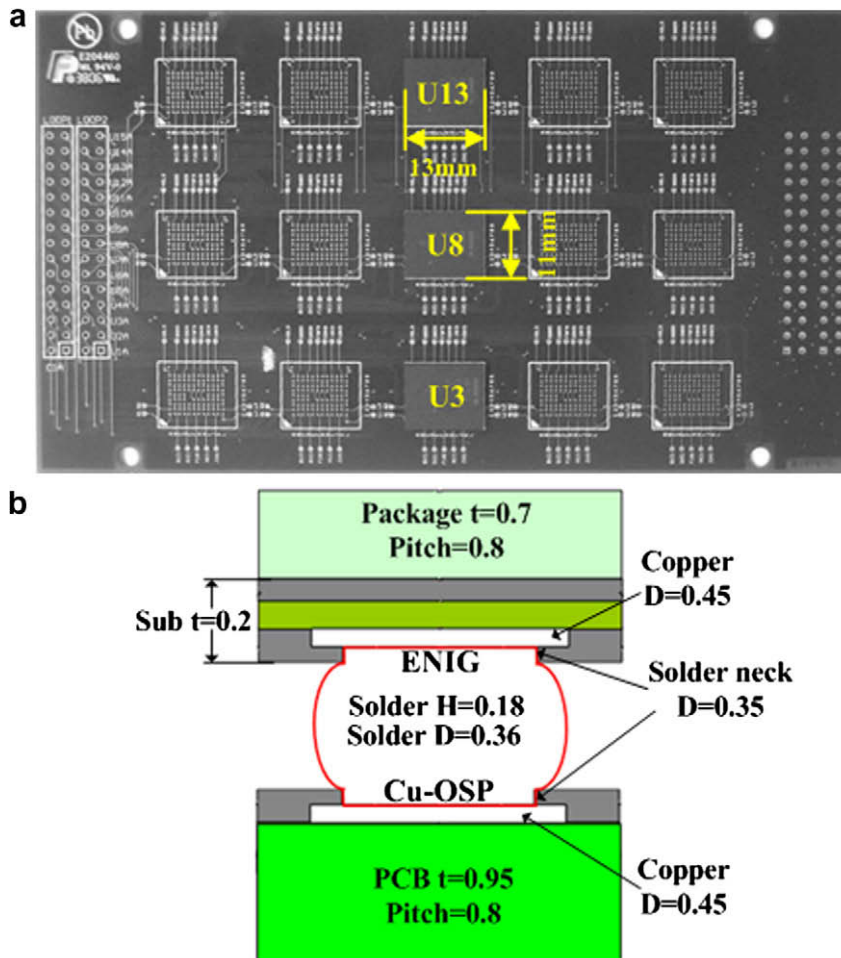


Fig. 1. Board-level package: (a) entire picture; (b) structural of solder interconnection.

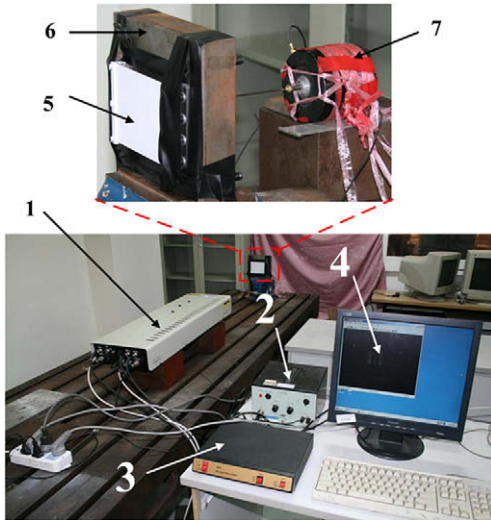


Fig. 3. Spot of modal test. (1 – VobroMap; 2 – power amplifier; 3 – analog video filter; 4 – monitor; 5 – board-level package; 6 – clamp; 7 – exciter.)

ies from 1 Hz to 2 kHz with a frequency interval of 1 Hz. Clear stripe pattern can be observed at the resonance frequencies. The stripe patterns are processed by the VibroMap software to obtain the 2D contour figures and the animated display. In order to get better measurement results, the natural frequency of the clamp is first calculated by the FEA. The first natural frequency of the clamp is 2298 Hz, which means that the vibration of the clamp has little effect on the measurement results of the board-level package since the maximum frequency is 2 kHz.

3. Equivalent finite element model

We have built the equivalent FE model using ANSYS as depicted in Fig. 4. Details of the copper wire, VIA, layer structure of the PCB

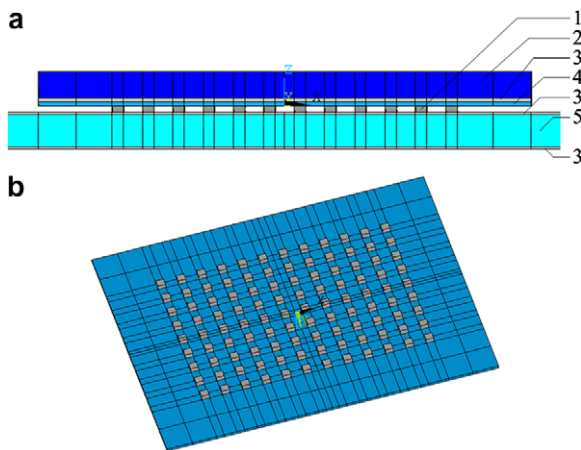


Fig. 4. FE model of board-level package. (1 – solder interconnection; 2 – package; 3 – solder mask; 4 – substrate; 5 – PCB.)

Table 1
Material parameters of board-level package.

	PCB	Solder mask	Solder interconnection	Substrate	Package
Young's modulus (Pa)	Orthotropic	5E + 9	4.25E + 10	2.1E + 10	2.7E + 10
Poisson's ratio	Orthotropic	0.47	0.4	0.25	0.3
Mass density (kg/m ³)	1910	1000	8410	1570	1035

were ignored in the equivalent FE model. Fixed boundary conditions were applied to the surfaces at the two opposed edges of the board-level package. This FE model contains 59,182 degrees of freedom and 44,624 linear hexahedral solid elements. Each solid element has eight nodes and each node has translational degrees of freedom in the *x*, *y* and *z* directions. It was shown in Ref. [13] that it is feasible to simplify the solder interconnection as a hexahedral block to reduce the computational size of the FE model; therefore, we adopted this strategy in this work.

In the FEA, all components including PCB, solder joints, substrate, pads and package, were assumed to be linear elastic materials. Also, the PCB was considered as a uniform transversely isotropic material. The initial input material properties of the PCB were extracted from Ref. [14] as listed in Tables 1 and 2. The Block Lanczos method is adopted to solve the mode shape and natural frequencies.

The mode shapes and natural frequencies of the board-level package depend greatly on the material properties of the PCB. As a result, the material properties of the PCB, including the Young's modulus (E_x , E_y and E_z), shear modulus (G_{xz} , G_{yz} and G_{xy}), Poisson's ratio (ν_{xz} , ν_{yz} and ν_{xy}) and mass density are taken as the design variables during the optimization of the equivalent material properties. The optimization process based on the Taguchi method is shown in Fig. 5. Equivalent materials properties that lead to the best fit between EMA and FEA results are taken as the optimized equivalent material properties.

In order to find the dominant material properties that affect the natural frequencies of the board-level package, each parameter was varied $\pm 10\%$ and the FEA results are as shown in Fig. 6. It can be seen that the Young's modulus in the *x* and *y* directions (E_x , E_y), shear modulus in the *xy* plane (G_{xy}) and the mass density have larger effects on the natural frequencies of the board-level package than others. Therefore, these four variables are adopted as the factors to be optimized using the Taguchi method.

The optimization process includes two steps: First, the four design variables are separately optimized with respect to the minimal average error of the first nine natural frequencies between the EMA and FEA results to reduce the range of the variables. Fig. 7 depicts changes of the average error of the first nine natural frequencies vs. the change of the design variables. The average error is defined by

$$RE = \sum_{i=1}^n \frac{|f_{EMA}(i) - f_{FEA}(i)|}{f_{EMA}(i) \cdot n} \times 100\% \quad (1)$$

where $f_{EMA}(i)$ is the *i*th natural frequency from EMA, $f_{FEA}(i)$ is the *i*th natural frequency from FEA. The natural frequencies obtained by EMA and FEA are in good agreement with an average error of

Table 2
Orthotropic properties of PCB.

E_x , E_y (Pa)	1.69E + 10	E_z (Pa)	0.74E + 10
G_{xz} , G_{yz} (Pa)	0.33E + 10	G_{xy} (Pa)	0.76E + 10
ν_{xz} , ν_{yz}	0.39	ν_{xy}	0.11

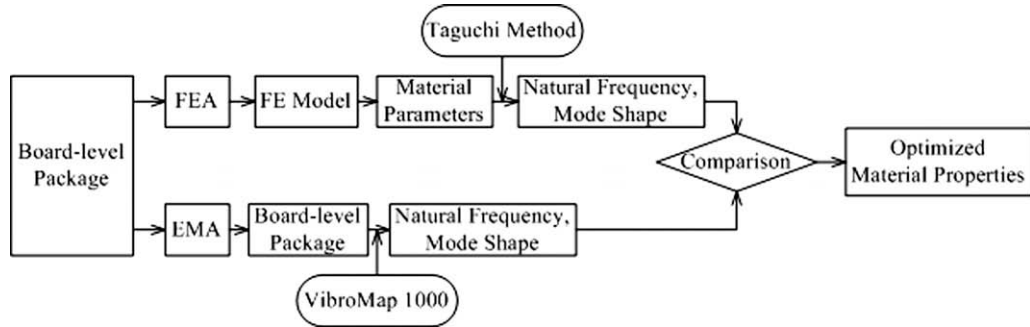


Fig. 5. Optimization process of material properties.

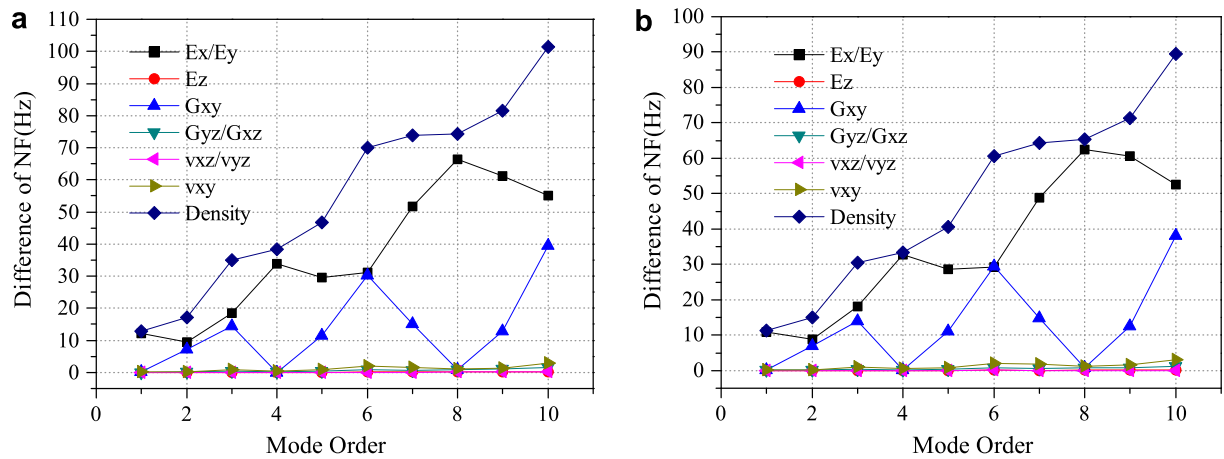


Fig. 6. Effect of material properties variation on natural frequencies: (a) decreasing 10%; (b) increasing 10%.

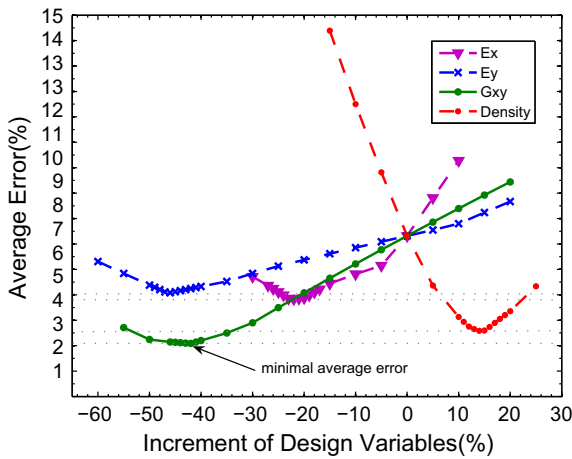


Fig. 7. Average error of the first nine frequencies.

Table 4
Taguchi table with four factors and three levels.

Group	1	2	3	4	5	6	7	8	9
<i>Factors</i>									
E_x	L_1	L_1	L_1	L_2	L_2	L_2	L_3	L_3	L_3
E_y	L_1	L_2	L_3	L_1	L_2	L_3	L_1	L_2	L_3
G	L_1	L_2	L_3	L_2	L_3	L_1	L_3	L_1	L_2
D	L_1	L_2	L_3	L_3	L_1	L_2	L_2	L_3	L_1

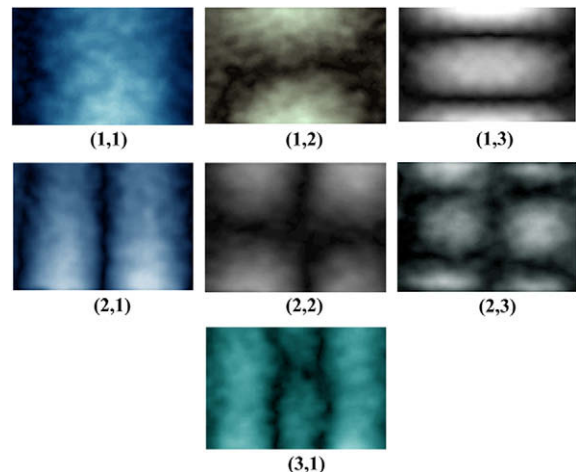


Fig. 8. Interferometric stripe figures: (a) (1, 1); (b) (1, 2); (c) (1, 3); (d) (2, 1); (e) (2, 2); (f) (2, 3); (g) (3, 1).

Table 3
Factors and levels for the optimization and experiment.

Notation	Factors	Level 1(-3%)	Level 2	Level 3(+3%)
E_x	E_x (Pa)	1.6393E + 10	1.6900E + 10	1.7407E + 10
E_y	E_y (Pa)	1.6393E + 10	1.6900E + 10	1.7407E + 10
G	G_{xy} (Pa)	4.2758E + 9	4.4080E + 9	4.5402E + 9
D	Density (kg/m^3)	1852.70	1910.00	1967.30

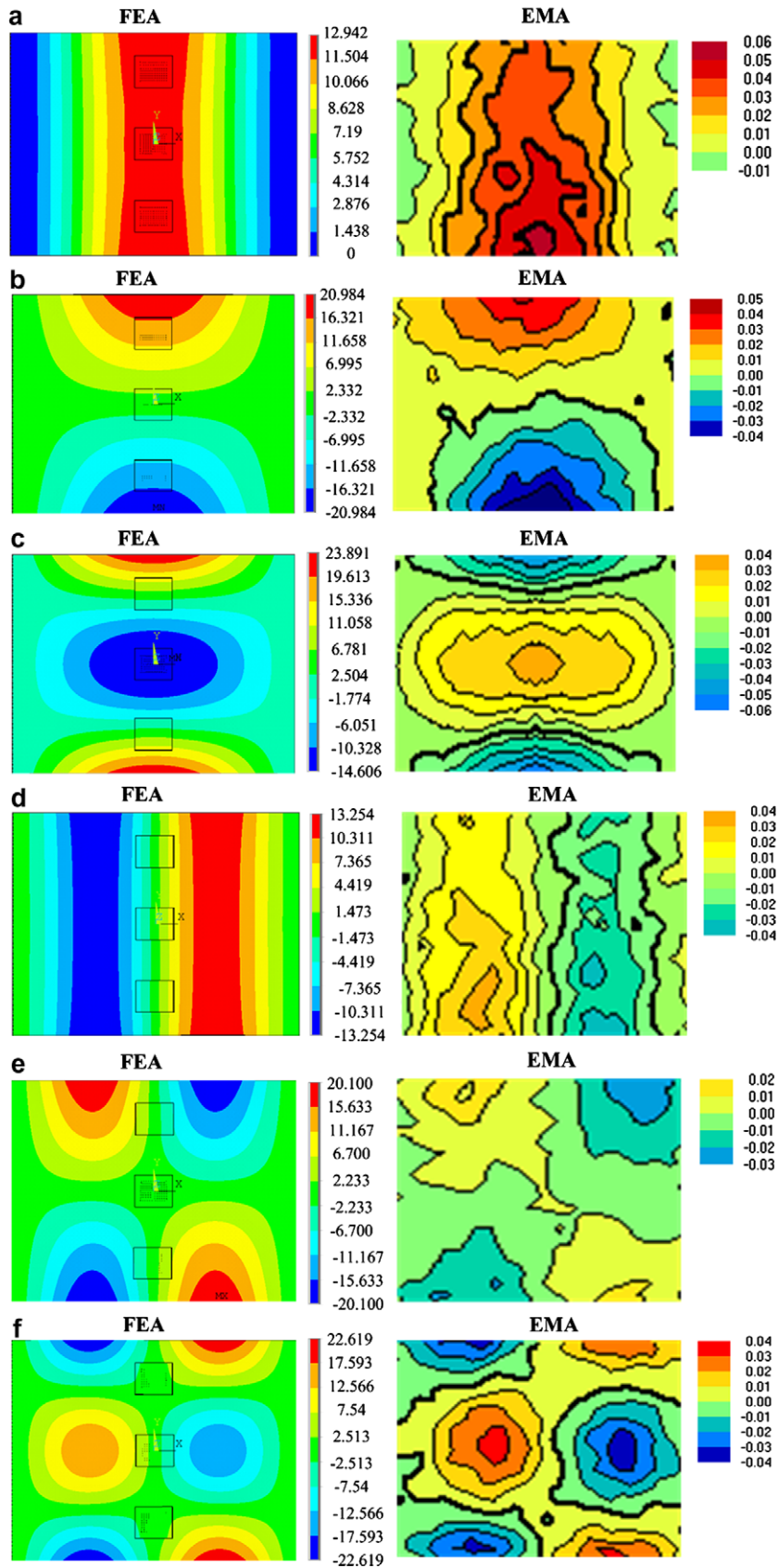


Fig. 9. Comparison between mode shapes of FEA and EMA: (a) (1, 1); (b) (1, 2); (c) (1, 3); (d) (2, 1); (e) (2, 2); (f) (2, 3); (g) (4, 1); (h) (3, 1); (i) (3, 2).

2.086% when the shear modulus in the xy plane (G_{xy}) decreases by 42%, which shows that the initial input of G_{xy} was the least accurate.

In the Taguchi method, every factor is divided into three levels. The factors selected and their levels used are listed in Table 3.

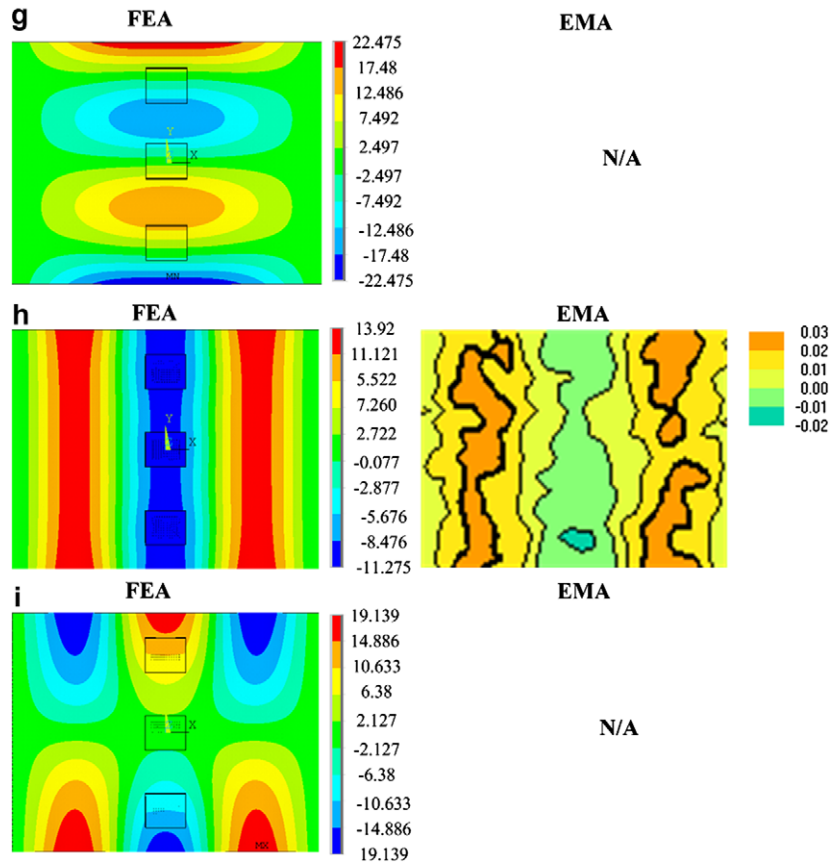


Fig. 9 (continued)

These different levels of parameters are listed in a $L_9 (3^4)$ orthogonal array, as shown in Table 4.

4. Results and discussion

The added-mass of the exciter will reduce the accuracy of the testing if it is attached on the surface of the board-level package. Therefore, the exciter was attached on the clamp in our experiments. It was found that different modal shapes could be excited

at different locations of the clamp. Fig. 8 shows the interferometric stripe patterns of modes (1, 1), (1, 2), (1, 3), (2, 1), (2, 2), (2, 3), (3, 1), and the measured corresponding resonant frequencies are 269 Hz, 326 Hz, 684 Hz, 755 Hz, 869 Hz, 1258 Hz and 1466 Hz, respectively. The dark region in the figures corresponds to the nodal lines of different modal shapes.

The interferometric stripe patterns could be processed to obtain 2D contour figures of these modes using the VibroMap software. Fig. 9 compares the corresponding mode shapes up to 2 kHz obtained by FEA and EMA. The measured mode shapes and simulated

Table 5
Average error between FEA and EMA.

	Group									
	Original material	Optimized material properties								
		1	2	3	4	5	6	7	8	9
Average error (%)	6.320	2.153	1.476	1.456	1.871	3.215	1.998	3.086	2.214	3.840

Table 6
Error of the first nine frequencies after optimization.

Mode	1st	2nd	3rd	4th	5th	6th	7th	8th	9th
<i>Natural frequencies (Hz)</i>									
EMA	269	326	684	755	869	1258	/	1466	/
FEA (original material properties)	277.11	364.11	728.94	762.28	925.28	1385.8	1501.1	1544.6	1681.5
FEA (optimized material properties)	269.74	328.23	665.3	741.77	859.45	1242.9	1435.9	1501.9	1591.9
<i>Error (%)</i>									
Original material properties	3.015	11.690	6.570	0.964	6.476	10.159	/	5.362	/
Optimized material properties	0.275	0.684	2.734	1.752	1.099	1.200	/	2.449	/

mode shapes using the optimized equivalent material properties are in good agreement.

We noticed certain degree of asymmetry in the measured 1st and 4th mode shapes, which was due to the nonuniform clamping at different locations of the board-level package. The 7th and 9th order modes could not be excited maybe due to the setup design used in our experiments. Table 5 shows the average error of the first nine natural frequencies between EMA and FEA. It can be seen that Group 3 reduces the average error from 6.32% to 1.456% compared with the initial input material properties. Table 6 lists some natural frequencies and the errors between FEA and EMA results before and after the optimization. The natural frequencies obtained by FEA and EMA are in good agreement with a global error less than 2%, while the error of the first natural frequency is less than 0.3%. Therefore, the third group material parameter in Table 5 is adopted as the optimized equivalent material properties to be used for the FEA of dynamic response of the board-level package.

5. Conclusion

A laser-based interferometric technique has been used in this investigation to measure the modal parameters of the board-level package. The 132 mm × 72 mm × 1 mm board-level package mounted with three 13 mm × 11 mm chip scale packages at the U3, U8 and U13 locations has been modeled using ANSYS. The equivalent material properties of the PCB have been obtained based on the minimization of the global error between EMA and FEA results. These optimized equivalent material properties can be used as input for the FEA in the future to study the dynamic response of the board-level package and the solder interconnections.

Acknowledgements

This work was supported in part by Natural Science Foundation of China under Grant 50905118 and 50805097, National High-tech

Research and Development Program (863 Program) Grant 2006AA4Z334.

References

- [1] Yeh Chang-Lin, Tsai Tsung-Yueh, Lai Yi-Shao. Transient analysis of drop responses of board-level electronic packages using response spectra incorporated with modal superposition. *Microelectron Reliab* 2007;47(12): 2188–96.
- [2] Yeh Chang-Lin, Lai Yi-Shao. Support excitation scheme for transient analysis of JEDEC board-level drop test. *Microelectron Reliab* 2006;46(2–4):626–36.
- [3] Yeh Chang-Lin, Lai Yi-Shao, Kao Chin-Li. Evaluation of board-level reliability of electronic packages under consecutive drops. *Microelectron Reliab* 2006;46(7):1172–82.
- [4] Zhu Li-Ping, Marcinkiewicz Walt. Drop impact reliability analysis of CSP packages at board and product levels through modeling approaches. *IEEE Trans Compon Pack Technol* 2005;28(3):449–56.
- [5] Shin Dong-Kil, Lee Duk-Yong, Ahn Eun-Chul, Kim Tae-Hun, Cho Tae-Je. Development of multi stack package with high drop reliability by experimental and numerical methods. In: *Proceedings – IEEE 56th electronic components and technology conference*; 2006. p. 377–82.
- [6] Luan Jing-En, Tee Tong-Yan, Pek Eric, Lim Chwee-Teck, Zhong Zhao-Wei, Zhou Jiang. Advanced numerical and experimental techniques for analysis of dynamic responses and solder joint reliability during drop impact. *IEEE Trans Compon Pack Technol* 2006;29(3):449–56.
- [7] Luan Jing-en, Tee Tong-Yan, Pek Eric, Lim Chwee-Teck, Zhong Zhao-Wei. Dynamic responses and solder joint reliability under board level drop test. *Microelectron Reliab* 2007;47(2–3):450–60.
- [8] Tee Tong-Yan, Ng Hun-Shen, Lim Chwee-Teck, Pek Eric, Zhong Zhao-Wei. Impact life prediction modeling of TFBGA packages under board level drop test. *Microelectron Reliab* 2004;44(7):1131–42.
- [9] Chong DYR, Che FX, Pang John HL, Ng Kellin, Tan Jane YN, Low Patrick TH. Drop impact reliability testing for lead-free and lead-based soldered IC packages. *Microelectron Reliab* 2006;46(7):1160–71.
- [10] Lee Ying-Chih, Wang Bor-Tsuen, Lai Yi-Shao, Yeh Chang-Lin, Chen Rong-Sheng. Finite element model verification for packaged printed circuit board by experimental modal analysis. *Microelectron Reliab* 2008;48(11–12):1837–46.
- [11] Zhang Bo, Ding Han, Sheng Xin-Jun. Modal analysis of board-level electronic package. *Microelectron Eng* 2008;85(3):610–20.
- [12] Optonor VibroMap 1000 user guide.
- [13] Ranouta Amarinder Singh, Fan XueJun, Han Qiang. Shock performance study of solder joints in wafer level packages. In: *International conference on electronic packaging technology & high density packaging*; 2009. p. 1266–76.
- [14] Lall Pradeep, Islam Mohd-Nokibul, Singh Naveen, Suhling Jeffrey C, Darveaux Robert. Model for BGA and CSP reliability in automotive underhood applications. *IEEE Trans Compon Pack Technol* 2004;27(3):585–93.